Hindawi
Advances in Civil Engineering
Volume 2019, Article ID 8763569, 15 pages
https://doi.org/10.1155/2019/8763569

Research Article

Numerical Experiments on Triaxial Compression Strength of Soil-Rock Mixture

Yanxi Zhao[1] **and Zhongxian Liu**[2]

[1]*School of Architectural Engineering, Nanjing Institute of Technology, Nanjing 211167, China*
[2]*Tianjin Key Laboratory of Civil Structure Protection and Reinforcing, Tianjin Chengjian University, Tianjin 300384, China*

Correspondence should be addressed to Yanxi Zhao; 249543863@qq.com

Received 15 August 2018; Revised 14 December 2018; Accepted 31 December 2018; Published 27 January 2019

Academic Editor: Claudio Mazzotti

Soil-rock mixture is a kind of unfavorable geologic material, and it is composed of low-strength soil particles and high-stiffness rock blocks. Mechanical properties of soil-rock mixture were controlled by the internal mesoscopic medium, thus resulting in great difficulties of determination of mechanical parameters. In this paper, influences of rock content, mesoscopic features, and random distribution of mixture in soil-rock mixture on its shear strength were discussed through discrete element numerical simulation of the laboratory triaxial test. Results demonstrated that, with the increase of rock content, the internal friction angle of soil-rock mixture increased continuously, while the cohesion of soil-rock mixture decreased firstly and then increased. The stress-strain curve belonged to a nonlinear hardening type, which was close to soil characteristic. However, the shear strength was affected by mesoscopic medium of mixture particles significantly, resulting in the strong discreteness of strength, and only by large amounts of data statistics can we get a better regularity of strength. The research results can provide references to determine mechanical parameters of soil-rock mixture.

1. Introduction

Soil-rock mixture is a kind of bad geological material, which is composed of low-strength soil particles and high-stiffness rock mass cementing. Its mechanical properties are controlled by mesoscopic medium and cementation degree in the medium, resulting in the great difficulties of determination of mechanical parameters. How to consider the mesoscopic structure of soil-rock mixture and then establish the method to determine its mechanical parameters have important theoretical and practical value.

Currently, mechanical parameters and deformation features of soil-rock mixture are mainly studied by the in situ test, laboratory test, and numerical simulation. Mechanical parameters and deformation characteristics were mainly controlled by mesoscopic structure of soil-rock mixture [1]. Miller et al. [2, 3] conducted triaxial laboratory tests on the mixture of clay and coarse sand and found that when the sand content was between 50% and 70%, with the increase of the sand content, the internal friction angle gradually increased, while the cohesive force gradually decreased. Kristensson and Ahadi [4] studied the shear failure characteristics of soil-rock mixture by using discrete element method and found that the failure characteristics were significantly affected by the shape of rubbles. Kuenza et al. [5] conducted torsional shear tests on soil-rock mixture and found that the soil-rock mixture strength was greatly affected by the soil-rock content. When the rock content was less than 40%, soil mass bored the major stress. When the rock content was more than 40%, the soil mass and rocks bore stress together. Irfan et al. [6, 7] studied the effect of coarse grain content on the strength of soil-rock mixture. Through laboratory experiments, they found that when the grain content was less than 10%, the shear strength had no effect with the increase of content. When the grain content was more than 30%, the shear strength of soil-rock mixture increased significantly with the increase of the content. When the grain content is between 10% and 30%, the shear strength is still dominated by fine grains, while the influence of coarse grains on shear strength is small.

In recent years, the study of mechanical properties of soil-rock mixture media with the help of numerical simulation technology has developed rapidly and has become an important method to study the mechanical properties of soil-rock mixture [8–12]. Two-dimensional strength test of soil-rock mixture mesoscopic medium can be realized by digital image processing technology and mixture random reconstruction technology. For instance, Tanshman et al. [13] applied numerical image processing and CT technology to study the concrete-asphalt mixture and gained the "microstructural tensor" of mixture distribution through a quantitative analysis. Yue et al. [14, 15] analyzed the internal mesoscopic structure of granite in Hong Kong by using digital image finite element analysis and established a mesoscopic model to study the mechanical properties. The three-dimensional strength test could be realized through three-dimensional CT scanning and three-dimensional random particle reconstruction. Shi et al. [16–19] studied the shape parameters of pebble and gravel particles by three-dimensional laser scanning. The results showed that, for the same volume of pebble and gravel, the smaller the volume, the smaller the surface area difference between pebble and gravel, and the smaller the influence of mechanical properties. The overall shape coefficient of pebble was generally higher than that of gravel. Then, the results of triaxial compression test or shear test are obtained. Next, they acquired results which conformed relatively well to mechanical properties of soil-rock mixture through a triaxial compression test and a shearing test.

In this paper, three-dimensional random particles were generated by the Fourier random formation method [20] based on the triaxial compression test. Subsequently, these particles and soil particles were compacted into the soil-rock mixture samples. A triaxial compression test of the sample was carried out to discuss influences of rock content and mesoscopic structure on strength of media. The research results will provide references for determination of strength parameters of the soil-rock mixture.

2. Laboratory Experiment

2.1. Experimental Materials and Processes. Soil-rock mixture was usually considered to be composed of "soil" and "block rock" binary media. Soil was used as matrix and rubble as filler. The soil used in the experiment was low liquid limit soil containing sand (particle size less than 10 mm), with water content 16%, liquid limit index 25.6%, and plastic index 12.6%. The gravel used in the experiment was artificial gravel (particle size 10–15 mm). The basic physical and mechanical parameters of soil and gravel are shown in Table 1.

The experiment was carried out on a medium triaxial experiment system (Figure 1). The confining pressure was 20 kPa, which ensured that the specimen was close to the rubber film and excluded the air. The method to saturate the sample was to gradually saturate the sample from the bottom to the top by opening the bottom inlet valve. The inlet valve was closed after the mixed sample was saturated, and drainage consolidation experiment was conducted according to the experiment requirements until the end of the experiment. The total mass of dry soil and

Table 1: Basic physical and mechanical parameters of soil and gravel.

Type	ρ (kg/m^3)	E (MPa)	μ	c (MPa)	φ (°)
Soil	2100	50.00	0.34	0.06	22
Gravel	2800	1.0E4	0.29	3	45

(a)

(b)

(c)

Figure 1: Triaxial test device for soil-rock mixture. (a) Medium triaxial test system. (b) Medium triaxial test sampler. (c) Gravel used in experiment.

gravel is 2960 g. The effects of stone content and different gravel types on the mechanical properties of soil-rock mixture were studied. The loading rate was 0.05 mm/min, and the loading should be stopped when the axial strain reached 15%.

2.2. Experiment Results. For different rock content experiments, gravel size was 10–15 mm (less than 10 mm particles are regarded as soil), stone content was 0% (gradation 1), 10% (gradation 2), 30% (gradation 3), 50% (gradation 4), and 70% (gradation 5), and the particle size distribution is shown in Table 2. The triaxial test results of soil-rock mixture are shown in Figure 2.

The results showed that (1) the stress-strain curve of soil-rock mixture was nonlinear, showing strong hardening characteristics; (2) under the same rock content, the greater the confining pressure, the higher the strength; (3) with the increase of rock content, the stress-strain curve fluctuated locally, indicating that the internal rubble structure was found to change, and there were extrusion and occlusion between them. The experimental results could provide a basis for subsequent numerical simulation.

3. Preparation of Numerical Samples

The numerical test was designed according to laboratory triaxial test system size (200 mm (height) × 101 mm (diameter)). Firstly, the random framework particle template is shown in Figure 3(a). The first row was gravel with good roundness, and the second row was the rock fragments which were commonly used in engineering. The third row was the very coarse cement particles. Different types of mixture templates can be used to construct particles randomly. The constructed particles were put in the constraint wall of the model in Figure 3(b). Then, the soil particles were generated outside the framework particles. The wall was composed of many triangle surfaces in the three-dimensional situations. During model generation, servo processing of samples was implemented through the upper and lower walls as well as the side walls. Next, the compression loading test was performed by controlling the upper and lower walls.

In the compression loading test, the upper wall moves downward slowly and the moving speed was controlled at 0.0005 m/s. The bottom wall was kept fixed in the test. During the compression, a constant confining pressure was applied on the side wall by the servo mechanism.

The soil particles were simulated by balls, and the rubble was basically nonbroken in the laboratory test, so the rubble was simulated by the nonbroken rigid cluster (clump). Sample preparation steps were introduced as follows:

(1) Firstly, soil particles with certain size were generated in PFC3D. To eliminate size effect, soil particles should be smaller than 1/80 of side length of the simulation device. Since the minimum side length was 101 mm, the soil particle diameter was smaller than 1.2 mm. In this paper, soil particle diameter was set 1.0–1.2 mm (Figure 4(a)).

(2) Based on the skeleton particle template (row 2) as shown in Figure 3(a), random rubbles were generated by using the random placement method in PFC3D, and the size range of rubble was 5–20 mm (as shown in Figure 4(b)).

(3) Because there was overlap between clumps of rubble and balls of soil particle, the simulation effect will be affected greatly. Therefore, after traversal of all balls, the ball that overlaps with clump was deleted, and then contact parameters were applied to contacts between particles in order to make soil-rock interaction bounce apart, and a 3D random mesostructure model of soil-rock mixture can be obtained for discrete element numerical simulation. Lastly the soil-rock mixture obtained by above procedure is shown in Figure 4(c).

4. Calibration of Soil-Rock Mesoscopic Parameters

During parameter calibration, macroscopic parameters of the material may not match with corresponding mesoscopic parameters. Changes of macroscopic parameters might induce changes of multiple mesoscopic parameters. There was a significant nonlinear relationship between macroscopic parameters and mesoscopic parameters. Hence, parameter calibration of PFC model was a very complicated process. During PFC model test, given determined size and combination mode of model particles, the mesoscopic parameters of the model need to be constantly adjusted. The calibration of the parameters was not completed until the macroscopic response of the model was close to the macroscopic parameters of the model we need, and the mesoscopic parameters obtained were the results required for calibration. In soil-rock mixture, there were three types of contacts, namely, soil-soil contact, soil-rock contract, and rock-rock contact. They were all simulated by the contact bonding model (CBM) [9]. Based on this model, it was suggested to adopt the following parameter calibration process:

(1) The material strength was set as a large value firstly, and then elasticity modulus of particles was adjusted. In other words, E_c was used to match macroscopic elasticity modulus of the material. Generally, mesoscopic elasticity modulus was positively correlated with macroscopic elasticity modulus. The normal and tangential rigidity ratio of particles was adjusted. This implies that k_n/k_s was used to match macroscopic Poisson's ratio of the material. Researches demonstrated that Poisson's ratio was positively correlated with the rigidity ratio. After several trials, the values of E_c and k_n/k_s were determined. Later, values of k_n and k_s could be gained from $k_n = 2E_c$.

Table 2: Gradation of soil-rock mixture with different stone contents.

Particle size (mm)	15~10	2~1	1~0.5	0.5~0.25	0.25~0.075	<0.075
Gradation 1 (%)	0	3.7	5.1	12.6	22	56.6
Gradation 2 (%)	10	3.3	4.6	11.3	19.8	51
Gradation 3 (%)	30	2.6	3.6	8.8	15.4	39.6
Gradation 4 (%)	50	2.0	2.6	6.3	11	28.3
Gradation 5 (%)	70	1.1	1.5	3.8	6.6	17.0

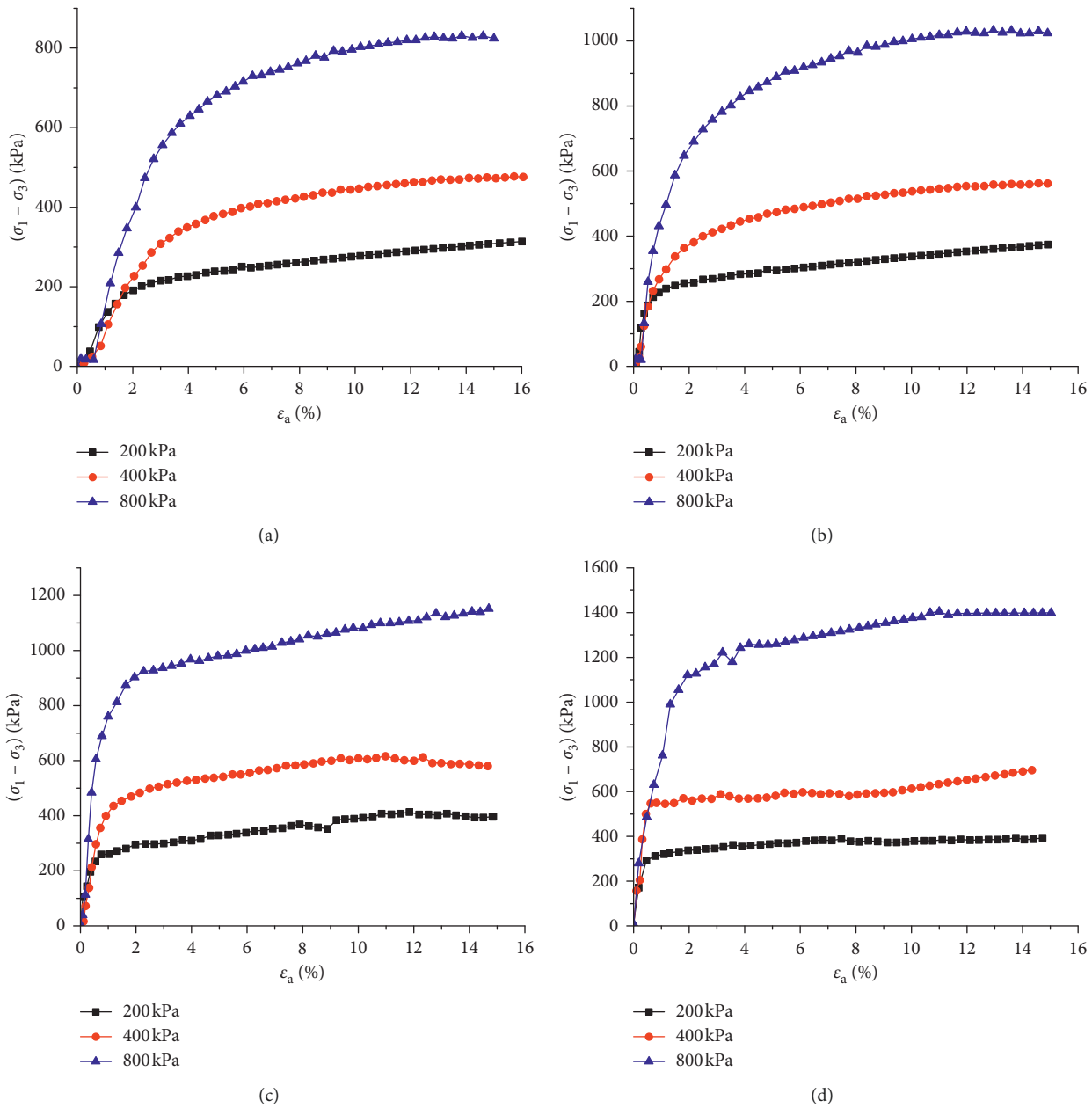

Figure 2: Continued.

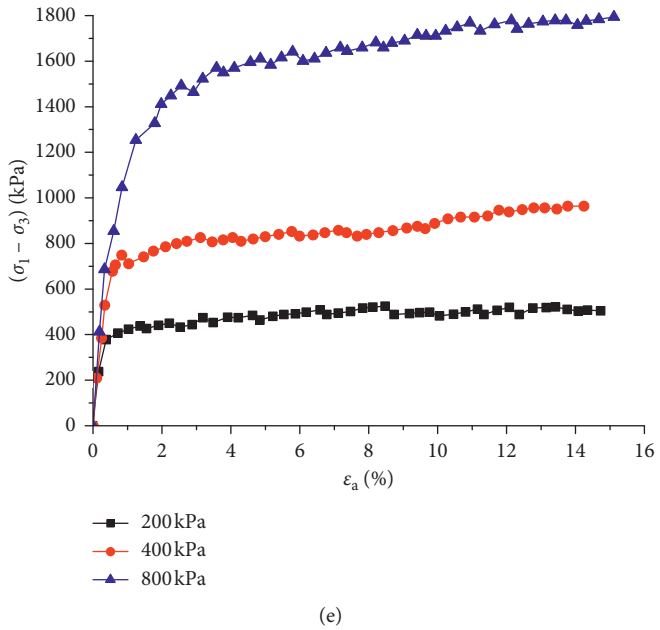

(e)

Figure 2: Stress-strain curves measured at different rock content. (a) 0%. (b) 10%. (c) 30%. (d) 50%. (e) 70%.

(a) (b)

Figure 3: Three-dimensional compression device. (a) Structure of different framework particles; (b) numerical test device.

(2) After obtaining the desired elastic response, the contact bond strength (σ_c and τ_c) between particles began to be calibrated, as they could influence the peak strength significantly, and the τ_c/σ_c may influence the failure mode of samples to some extent; generally, τ_c/σ_c was determined 1.0, and through continuous trials, σ_c and τ_c could be gained at matching of peak strength.

(3) Through calibration of previous two steps, the mesoscopic parameters before the peak strength of the material in the compression process could be matched. If it has to reproduce postpeak behavior of materials, the friction coefficient (μ) of particles had to be adjusted; however, there was no appropriate valuation standard of this parameter at present.

Based on calibration of pure soil according to above methods, rubble parameters were calibrated by the method proposed by Yoon [21]. Finally, the soil-rock mesoscopic parameters are listed in Table 3.

Numerical simulation studies of soil-rock mixture samples with 30% rock content under three confining pressures (200 kPa, 400 kPa and 800 kPa) were carried out and compared with laboratory test. It could be seen from Figure 5 that the stress-strain curves in all numerical simulation studies were basically consistent with those of the laboratory test. In the initial elastic stage, numerical simulation results were slightly smaller than laboratory test results, which indicated that the mesoscopic mechanical parameters can reflect deformation features of soil-rock mixture reasonably.

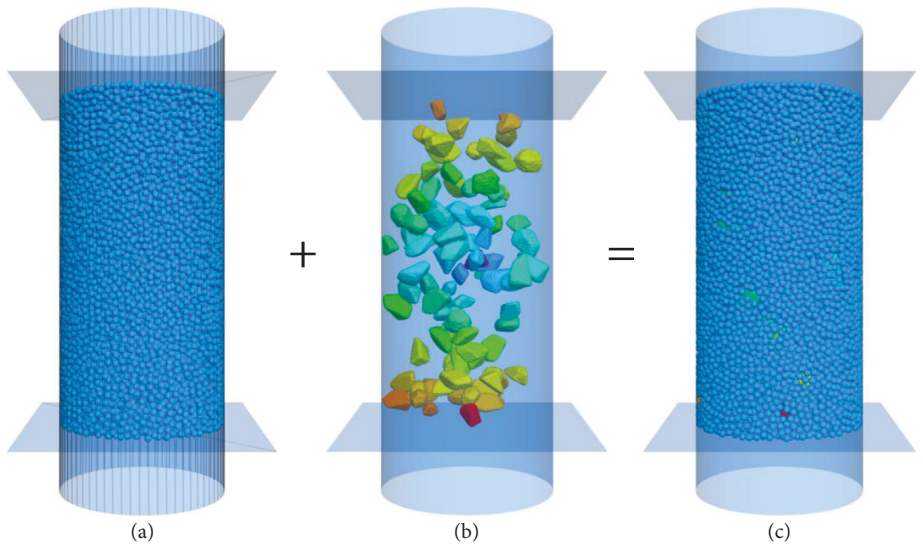

Figure 4: Generation of soil-rock mixture. (a) Pure soil particles; (b) rubble; (c) soil-rock mixture.

Table 3: Mesoscopic parameters of materials.

Contact type	Density (kg/m^3)	Stiffness (N/m)		Cohesion (N/m)		Friction coefficient
	ρ	k_n	k_s	F_n^b	F_s^b	μ
"Soil" (soil-soil and soil-rubble contact)	2000	4*e*6	2*e*6	6.0*e*2	6.0*e*2	0.45
"Rubble" (rubble-rubble contact)	2700	4*e*7	4*e*7	2.0*e*6	2.0*e*6	1.0

5. Analysis of Numerical Results

5.1. Effects of Rock Content. Figure 6(a) is the stress-strain curve and particle position at different strains with 30% rock content and confining pressure 400 kPa. Among them, balls (to simulate soil) showed displacement and clumps (to simulate gravel) showed rotation angle. As can be seen from the Figures 6(b)–6(e), with the increase of strain from 0 to 12%, the gravel acting as coarse skeleton would turn around 9°. Through the adjustment of its position, the contact between the coarse skeleton and soil particles became more dense, which further improved the bearing capacity and formed the hardening curve as shown in Figure 6(a).

On this basis, soil-rock mixture samples with rock contents of 0%, 10%, 20%, 30%, 40%, 50%, 60%, and 70% were simulated. The stress-strain curves are shown in Figure 7. In the initial loading stage, stress-strain curves were straight. Given the same rock content, strength was positively with confining pressure. Soil-rock mixture developed hardening features, and the hardening phenomenon increased significantly with the increase of confining pressure.

5.2. Effects of Coarse Aggregate Particle Shape. In order to discuss the effects of rock content on mechanical properties of soil-rock mixture, soil-rock mixture samples with different coarse degrees and rock contents of 0%, 10%, 20%, 30%, 40%, 50%, 60%, andlf 70% were simulated under the same rubble gradation. As shown in Figure 8, five groups of numerical model were constructed to each of rock content and confining pressure were set 200 kPa, 400 kPa and 800 kPa. Statistics on each group of cohesion and friction angle are shown in Table 4.

Based on organization of data in Table 4, the variation curves of cohesion and friction angle of soil-rock mixture with rock content are shown in Figure 9.

Figure 9 demonstrates that, with the increase of rock content, the internal friction angle of soil-rock mixture increased continuously, while the cohesion of soil-rock mixture decreased firstly and then increased. With the increase of the stone content, the extrusion and biting effect between the stones was significant, and the internal friction angle increased significantly. The specific performance was that, when the stone content increased from 0% to 70%, the internal friction angle increased from 16.0 to 35.6 and increased by 122.5%. When the stone content of soil-rock mixture increased from 0% to 50%, the cohesion decreased from 48.2 kPa to 20.6 kPa, which decreased by 57.3%. This was mainly because soil mass bored most stresses under low rock content, and the adding of rock fragment would decrease cohesion to some extent. When the rock content increased from 50% to 70%, the cohesion of soil-rock mixture increased by 65.5% from 20.6 kPa to 34.1 kPa. Under this circumstance, the increase of cohesion was mainly due to the significant effect of occlusion and extrusion between crushed stones at high stone content, which

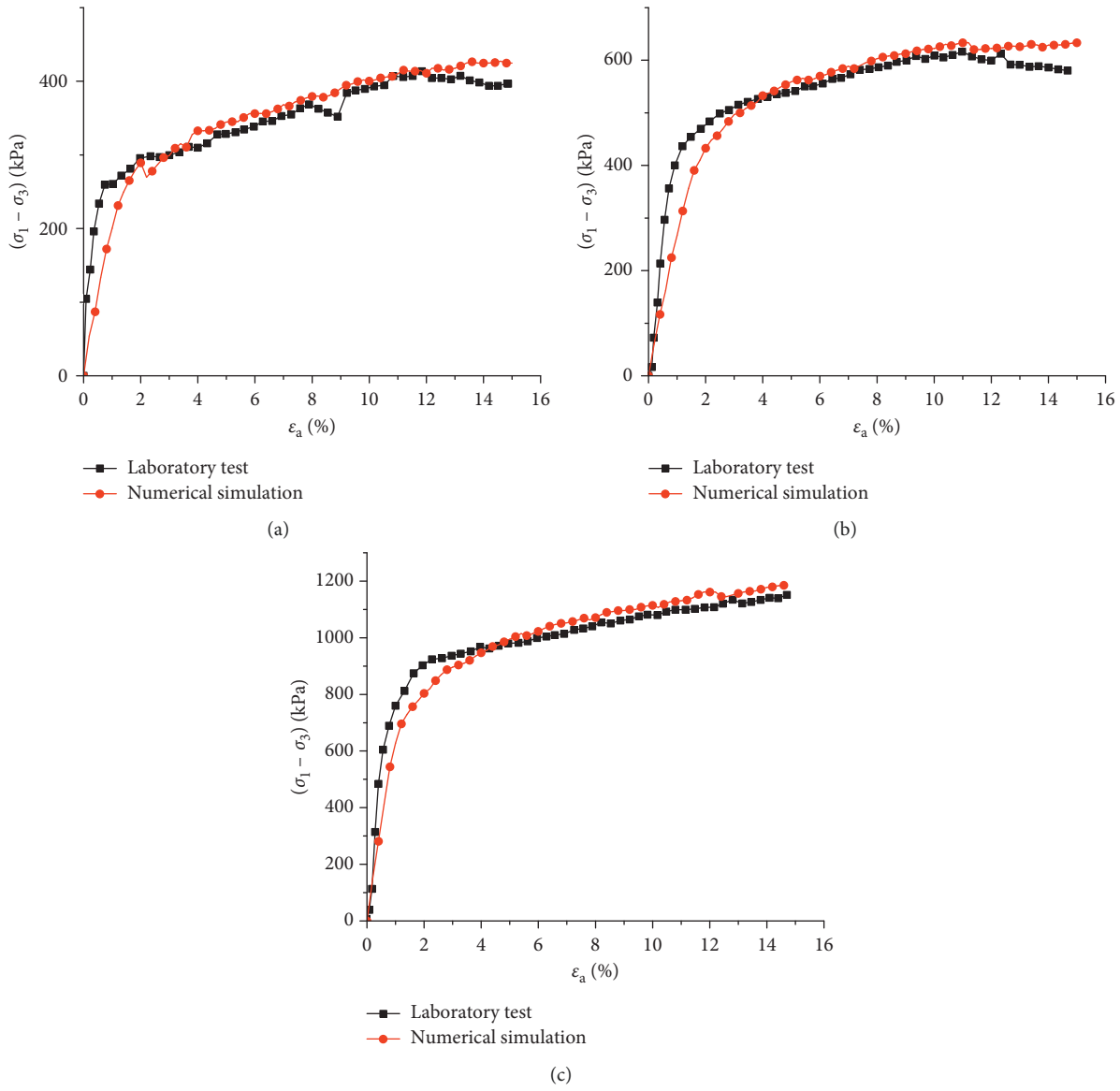

Figure 5: Variation laws of stress-strain curves under different confining pressures: (a) 200 kPa; (b) 400 kPa; (c) 800 kPa.

improved the cohesion index to a certain extent. The law of numerical simulation was basically consistent with that obtained by some scholars' experiments, which showed that the particle discrete element method had a good effect in simulating soil-rock mixture.

5.3. Effects of Rubble Random Position. The strength and mechanical properties of the soil-rock mixture at the same location were very discrete with the spatial distribution of the rubble. In this paper, mechanical properties of soil-rock mixture at different random positions of rock fragments were analyzed, the rock content of samples was controlled 30%, and the rock fragment size was 10–15 mm; three groups of random position models are shown in Figure 10 and the stress-strain curves are shown in Figure 11.

It can be found from Figure 11 that (1) the stress-strain curves of soil-rock mixture takes a nonlinear change, showing a strong hardening characteristic; (2) for the same sample, the strength was proportional to the confining pressure; (3) with the increase of confining pressure, the stress-strain curves fluctuated locally, and the results showed that the internal structure of the rock had changed, and the effect of extrusion and occlusion was strengthened. Peak strengths at different random positions under different confining pressures are listed in Table 5. As can be seen from the table, the peak strength of the same sample presented linear change with the confining pressure, and the higher the confining pressure was, the higher the peak strength was. Under the same confining pressure and different random positions, the peak strength had a certain dispersion.

The strength Mohr's circle and strength envelope lines of different samples under different random positions are shown in Figure 12. Strength indexes of soil-rock mixture

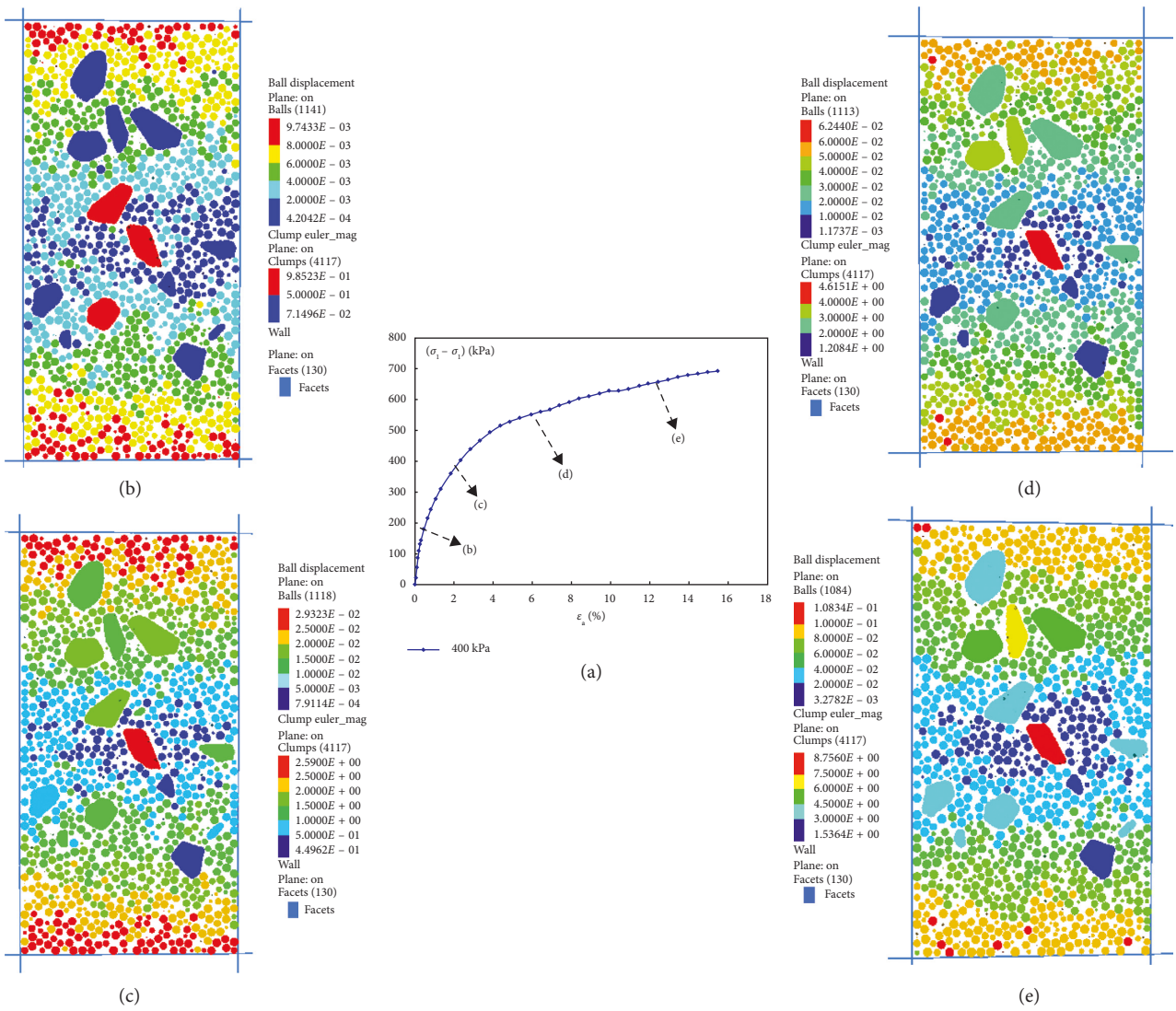

FIGURE 6: Particle position changes during compression: (a) stress-strain curve; (b) particle position at 1% strain; (c) particle position at 3% strain; (d) particle position at 6% strain; (e) particle position at 12% strain.

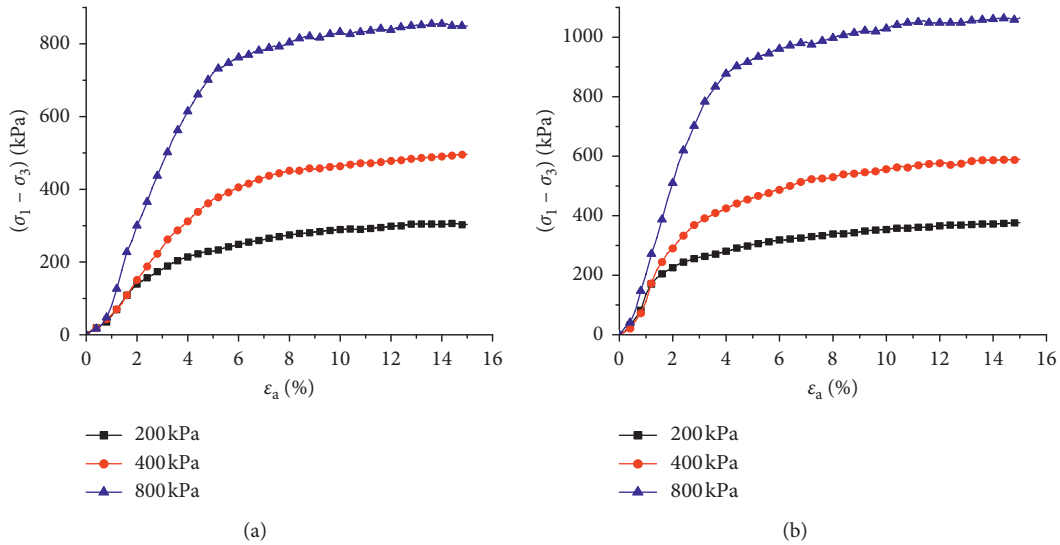

FIGURE 7: Continued.

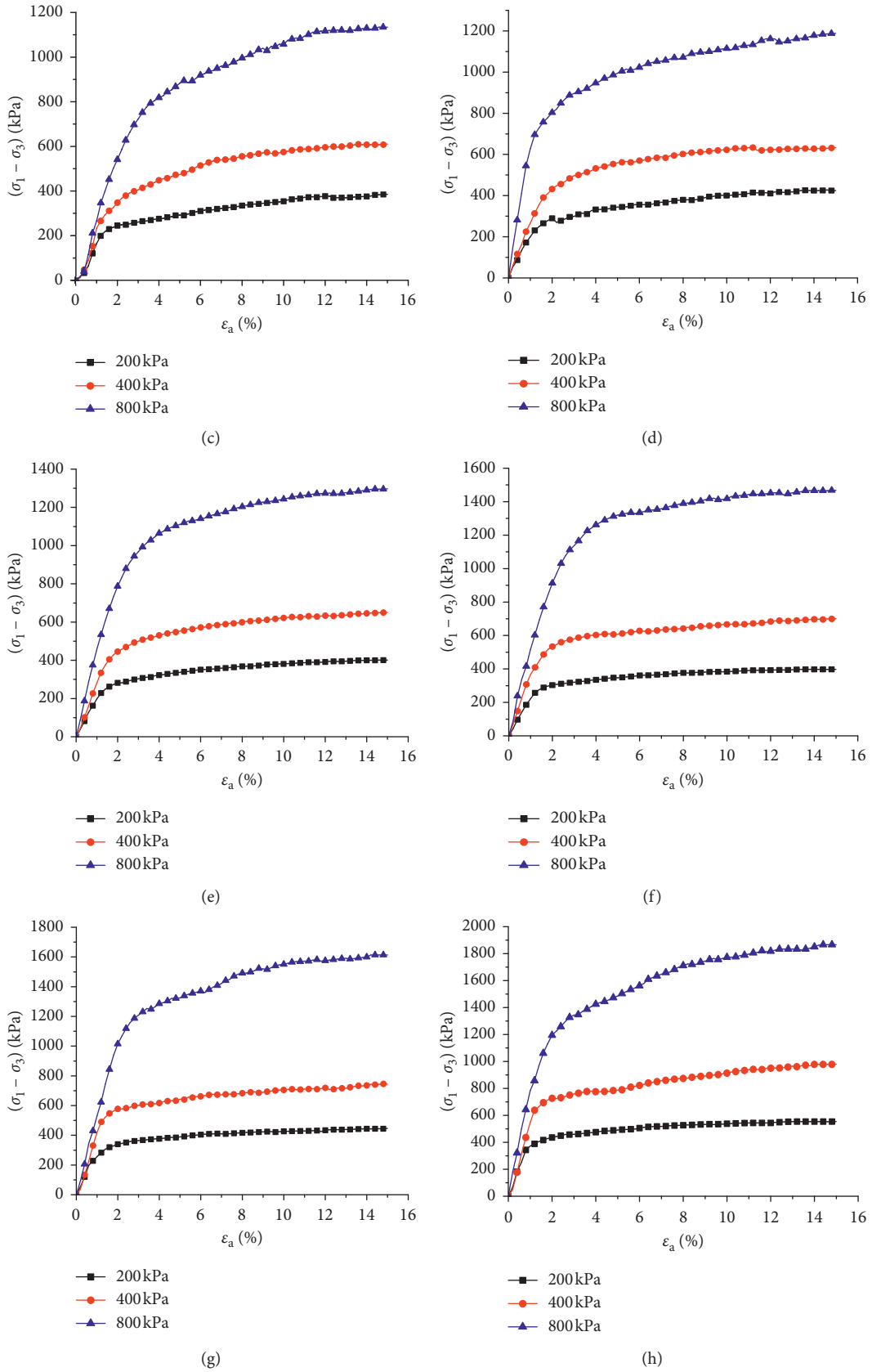

Figure 7: Stress-strain curves of samples with different rock contents: (a) 0%, (b) 10%, (c) 20%, (d) 30%, (e) 40%, (f) 50%, (g) 60%, and (h) 70%.

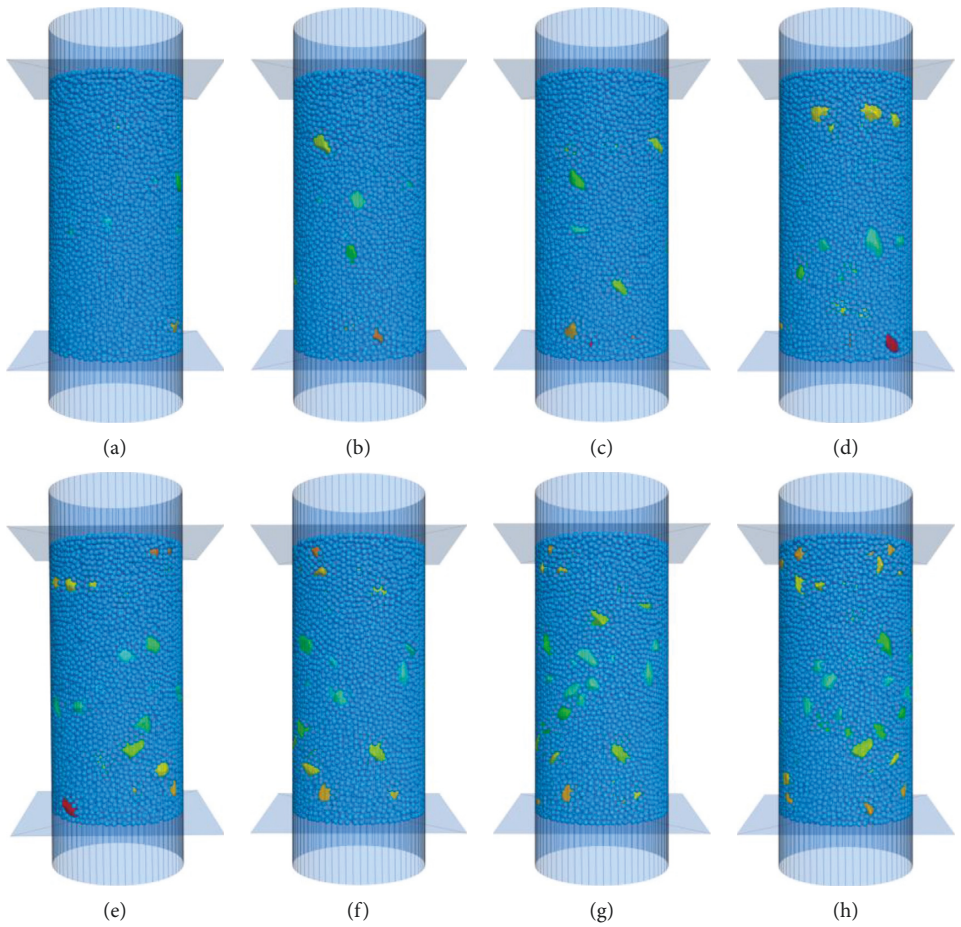

Figure 8: Models of different rock contents: (a) 0%, (b) 10%, (c) 20%, (d) 30%, (e) 40%, (f) 50%, (g) 60%, and (h) 70%.

Table 4: Statistics of strength parameters of different rock contents.

Number	Rock content (%)	φ (°)	c (kPa)
1	0	18.2	50.6
2	0	15.5	53.5
3	0	14.5	46.2
4	0	16.4	44.7
5	0	15.3	45.8
Average value	0	16.0	48.2
1	10	20.3	40.2
2	10	18.4	41.3
3	10	18.3	38.5
4	10	19.5	43.9
5	10	19.8	45.1
Average value	10	19.3	41.8
1	20	22.1	37.8
2	20	20.6	36.7
3	20	21.8	37.2
4	20	20.7	35.9
5	20	21.2	38.7
Average value	20	21.3	37.3
1	30	24.0	29.8
2	30	23.4	28.4
3	30	25.2	32.2
4	30	24.6	30.5
5	30	25.1	31.2
Average value	30	24.5	31.2
1	40	28.3	25.4
2	40	26.6	26.1
3	40	25.7	24.2
4	40	26.6	25.1
5	40	27.1	24.1
Average value	40	26.9	24.3
1	50	28.1	20.5
2	50	28.4	22.8
3	50	26.3	19.6
4	50	27.9	21.7
5	50	29.1	18.3
Average value	50	28.0	20.6
1	60	31.2	25.6
2	60	31.8	27.1
3	60	30.5	24.2
4	60	29.8	25.4
5	60	32.4	23.9
Average value	60	31.1	25.2
1	70	35.5	30.5
2	70	36.1	34.2
3	70	34.2	38.4
4	70	36.8	35.6
5	70	35.4	31.7
Average value	70	35.6	34.1

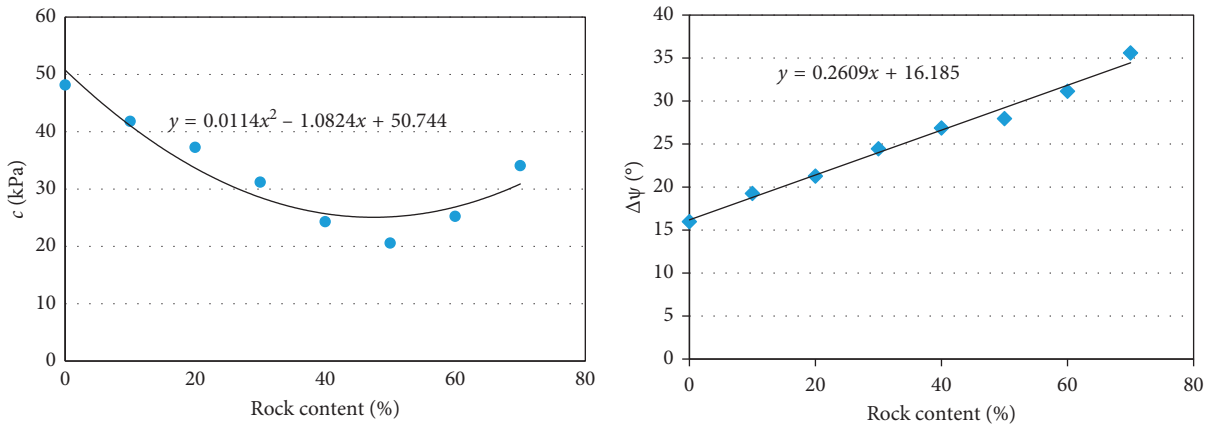

Figure 9: Variation laws of shear strength of soil-rock mixture with rock contents: (a) cohesion; (b) internal friction angle.

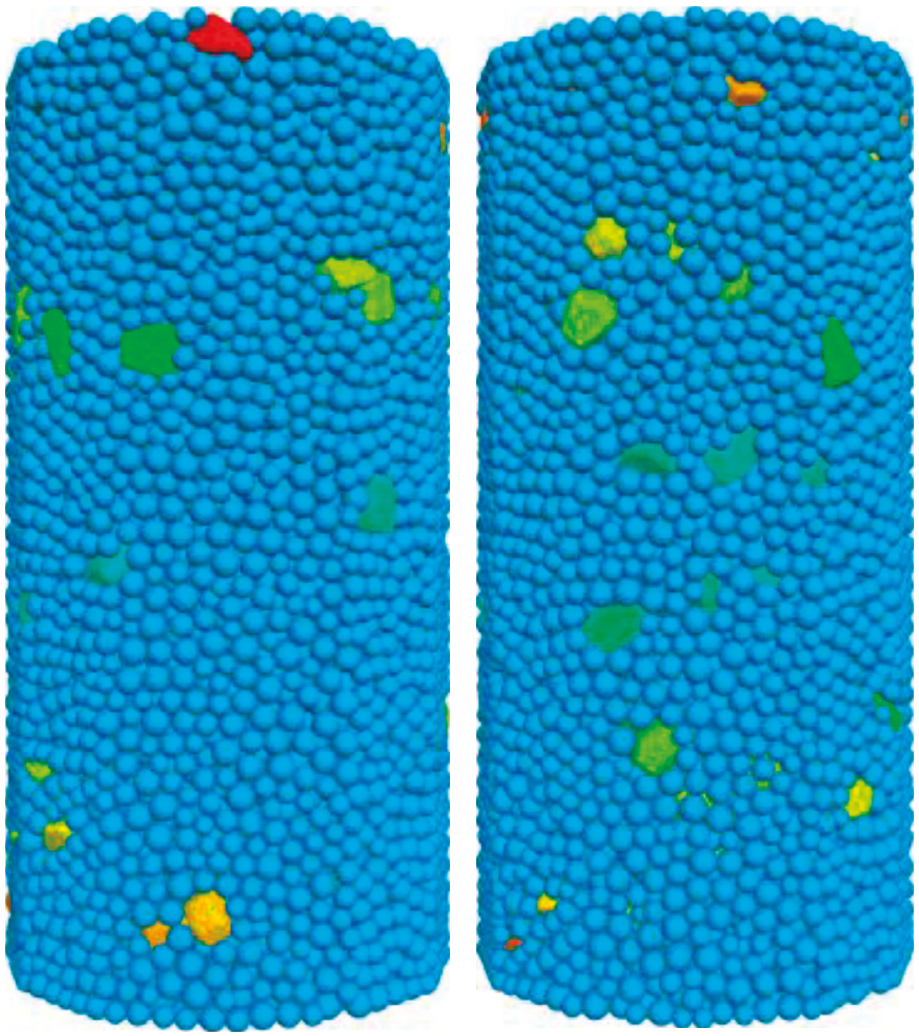

Figure 10: Continued.

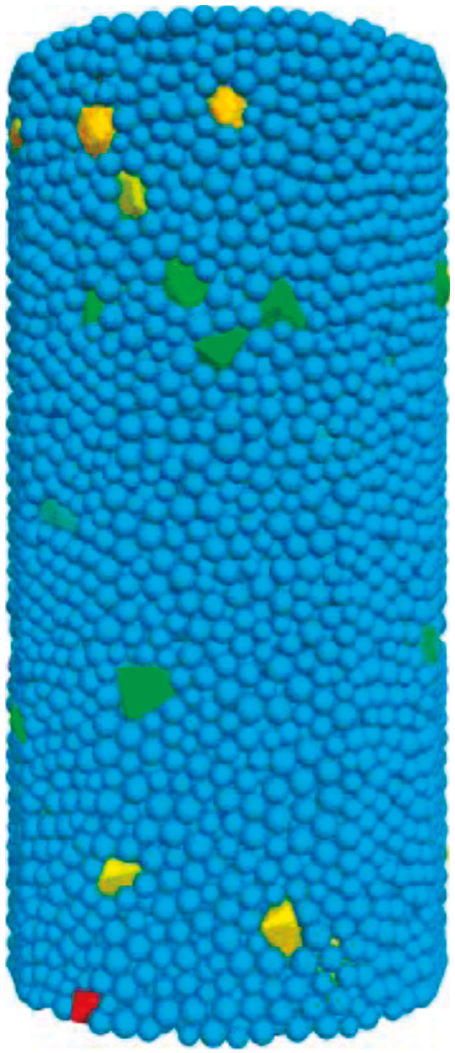

(c)

Figure 10: Three-dimensional model of rubble spatial random location distribution under the same rock content: (a) random position 1; (b) random position 2; (c) random position 3.

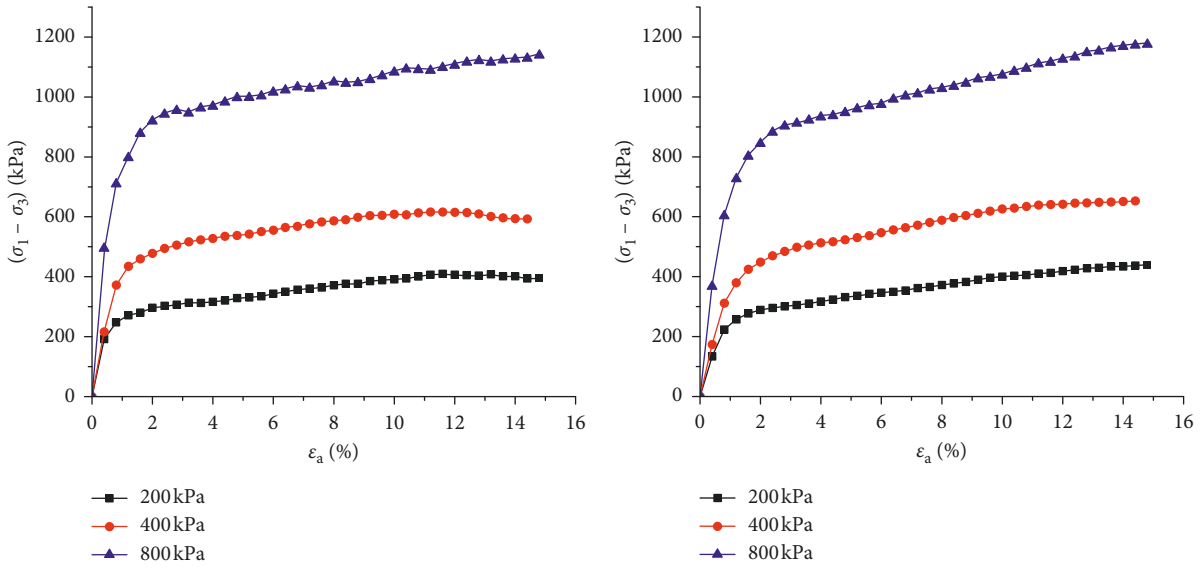

Figure 11: Continued.

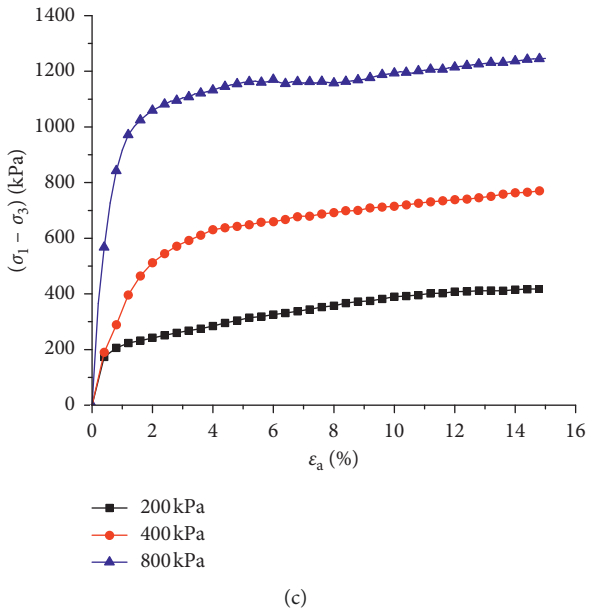

(c)

Figure 11: Stress-strain relationship of samples under different random positions: (a) random position 1; (b) random position 2; (c) random position 3.

Table 5: Peak strengths at different random positions under different confining pressures.

Random position	Confining pressures (kPa)		
	200 Peak strength (kPa)	400 Peak strength (kPa)	800 Peak strength (kPa)
Random position 1	414.23	618.11	1157.39
Random position 2	438.82	651.77	1175.41
Random position 3	417.86	764.29	1239.29

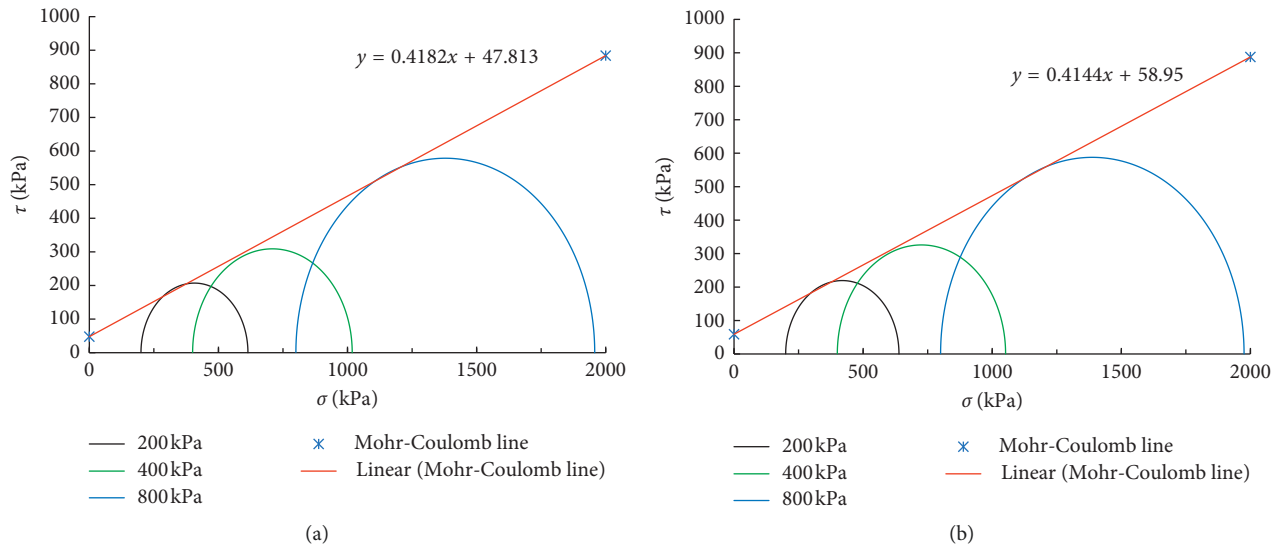

(a) (b)

Figure 12: Continued.

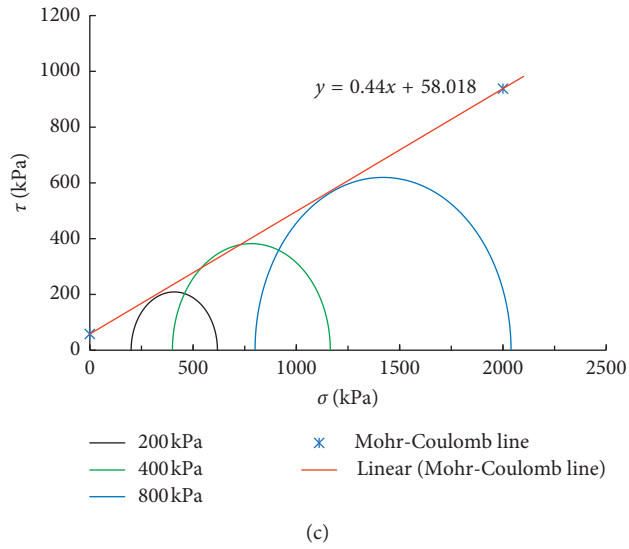

(c)

Figure 12: Mohr's circle and strength envelope lines of samples under different random positions: (a) random position 1; (b) random position 2; (c) random position 3.

Table 6: Strength indexes of soil-rock mixture under different random positions.

Random position	φ (°)	c (kPa)
Random position 1	22.69	47.81
Random position 2	22.51	58.95
Random position 3	23.75	58.01

under different random positions of gravel are listed in Table 6.

It can be seen from Table 6 that numerical values of friction angle were similar among three groups of samples. The difference between maximum and minimum of friction angle was only 6%. The difference between maximum and minimum of cohesion was 21.3%. It showed that the numerical simulation of mesoscopic skeleton particles of random soil-stone mixture was reliable, and the position of random aggregate would not cause great deviation of strength parameters.

6. Conclusions

Based on the conventional triaxial test of soil-rock mixture, this paper carried out a triaxial compression simulation test of the soil-rock mixture by using particle flow code (PFC). The influences of rock content, aggregate microscopic characteristics, and random distribution on macroscopic shear strength characteristics were analyzed, and the main conclusions are as follows:

(1) With the increase of rock content, the internal friction angle of soil-rock mixture increased continuously and the cohesion between them decreased firstly and then increased. Moreover, extrusion and occlusion effect of rubbles intensified gradually, while the internal friction angle increased dramatically.

(2) The variation law of friction angle of the soil-rock mixture was basically consistent with conclusions of Jia Xueming. It was discovered from the comparison between numerical simulation results and laboratory test results that the stress-strain curves of numerical simulation were basically consistent with those of the laboratory test. The stress-strain curves were hardening curves without evident peak strength.

(3) Although soil-rock mixture had certain discretion, the error was small, and it showed that the numerical simulation of the strength characteristics of the soil-rock mixture by the particle flow code had good credibility.

Data Availability

The data used to support the findings of this study are available from the corresponding author upon request.

Conflicts of Interest

The authors declare that there are no conflicts of interest regarding the publication of this paper.

Acknowledgments

This research was financially supported by the Natural Science Foundation of Jiangsu Province (BK20150726), the high level introduction talent scientific research start funds of Nanjing Institute of Technology (YKJ201430), and National Natural Science Foundation of China (51278327, 51808283).

References

[1] Y. C. Zhou, B. D. Wright, R. Y. Yang, B. H. Xu, and A. B. Yu, "Rolling friction in the dynamic simulation of sandPile

formation," *Physica A: Statistical Mechanics and its Applications*, vol. 269, no. 2–4, pp. 536–553, 1999.

[2] E. A. Miller and G. F. Sowers, "The strength characteristics of soil-mixture mixture," *Highway Research Board Bulletin*, vol. 183, pp. 16–23, 1957.

[3] H. Kawakami and H. Abe, "Shear characteristics of saturated gravelly clays," *Proceedings of the Japan Society of Civil Engineers*, vol. 1970, no. 183, pp. 55–62, 1970.

[4] O. Kristensson and A. Ahadi, "Numerical study of localization in soil systems," *Computers and Geotechnics*, vol. 32, no. 8, pp. 600–612, 2005.

[5] K. Kuenza, I. Towhata, R. P. Orense, and T. H. Wassan, "Undrained torsional shear tests on gravelly soils," *Landslides*, vol. 1, no. 3, pp. 185–194, 2004.

[6] T. Irfan and K. Tang, *Effect of the Coarse Fractions on the Shear Strength of Colluvium*, Geotechnical Engineering Office, Civil Engineering Department, Toronto, ON, USA, 1993.

[7] S. Huang, X. Ding, Y. Zhang, and W. Cheng, "Triaxial test and mechanical analysis of rock-soil aggregate sampled from natural sliding mass," *Advances in Materials Science and Engineering*, vol. 2015, Article ID 238095, 14 pages, 2015.

[8] M. J. Jiang, S. Leroueil, and J. M. Konrad, "Insight into shear strength functions of unsaturated granulates by DEM analyses," *Computers and Geotechnics*, vol. 31, no. 6, pp. 473–489, 2004.

[9] D. O. Potyondy and P. A. Cundall, "A bonded-Particle model for rock," *International Journal of Rock Mechanics and Mining Sciences*, vol. 41, no. 8, pp. 1329–1364, 2004.

[10] U. E. Shamy and M. Zeghal, "A micro-mechanical investigation of the dynamic resPonse and liquefaction of saturated granular soils," *Soil Dynamics and Earthquake Engineering*, vol. 27, no. 8, pp. 712–729, 2007.

[11] T. G. Sitharam, "Discrete element modelling of cyclic behaviour of granular materials," *Geotechnical and Geological Engineering*, vol. 21, no. 4, pp. 297–329, 2003.

[12] C.-L. Tang, J.-C. Hu, M.-L. Lin et al., "The Tsaoling landslide triggered by the Chi-Chi earthquake, Taiwan: insights from a discrete element simulation," *Engineering Geology*, vol. 106, no. 1-2, pp. 1–19, 2009.

[13] L. Tanshman, E. Masad, J. D'Angelo, J. Bukowski, and T. Harman, "X-ray tomography to characterize air void distribution in superpave gyratory compacted specimens," *International Journal of Pavement Engineering*, vol. 3, no. 1, pp. 19–28, 2002.

[14] Z. Q. Yue, S. Chen, and L. G. Tham, "Finite element modeling of geomaterials using digital image processing," *Computers and Geotechnics*, vol. 30, no. 5, pp. 375–397, 2003.

[15] D. KemPthorne and M. D. Myers, *The Landslide Handbook: A Guide to Understanding Landslides*, U.S. Geological Survey, Reston, VA, USA, 2008.

[16] C. Shi, J.-L. Shen, W.-Y. Xu, R.-B. Wang, and W. Wang, "Micromorphological characterization and random reconstruction of 3D particles based on spherical harmonic analysis," *Journal of Central South University*, vol. 24, no. 5, pp. 1197–1206, 2017.

[17] C. Shi, D.-J. Li, W.-Y. Xu, and R. Wang, "Discrete element cluster modeling of complex mesoscopic particles for use with the particle flow code method," *Granular Matter*, vol. 17, no. 3, pp. 377–387, 2015.

[18] C. Shi and J. Bai, "Compositional effects and mechanical parametric analysis of outwash deposits based on the randomised generation of stone blocks," *Advances in Materials Science and Engineering*, vol. 2015, Article ID 863915, 13 pages, 2015.

[19] C. Shi, S.-N. Wang, L. Liu, Q.-X. Meng, and Q. Zhang, "Mesomechanical simulation of direct shear test on outwash deposits with granular discrete element method," *Journal of Central South University*, vol. 20, no. 4, pp. 1094–1102, 2013.

[20] G. Mollon and J. Zhao, "Generating realistic 3D sand particles using Fourier descriptors," *Granular Matter*, vol. 15, no. 1, pp. 95–108, 2012.

[21] J. Yoon, "Application of experimental design and optimization to PFC model calibration in uniaxial compression simulation," *International Journal of Rock Mechanics and Mining Sciences*, vol. 44, no. 6, pp. 871–889, 2013.